

DPSK Transmission Through Silicon Microring Switch for Photonic Interconnection Networks

Lin Xu, Johnnie Chan, Aleksandr Biberman, Hugo L. R. Lira, Michal Lipson, and Keren Bergman

Abstract—We experimentally demonstrate for the first time switching of differential-phase-shift-keyed (DPSK) signals through a silicon photonic electrooptic microring switch. DPSK format has been shown to be robust to nonlinear effects, and has 3-dB improved receiver sensitivity with balanced detection compared to the on-off-keyed format. Moreover, an extension to multilevel phase-shift-keyed (PSK) format enables higher data bandwidth. Packetized transmissions of single- and multichannel 10-Gb/s DPSK signals are demonstrated. Error-free transmission and power penalties of less than 1.7 dB are achieved for all the examined wavelength channels, confirming format transparency of the microring switch for PSK format, and validating the use of DPSK signaling for photonic interconnection networks.

Index Terms—Differential-phase-shift keying (DPSK), electrooptical devices, microring resonators, packet switching.

I. INTRODUCTION

SILICON photonic technology presents a promising platform for solving the bandwidth and energy challenges associated with future chip-scale interconnects by offering higher bandwidth density, lower power consumption, and shorter latencies than traditional electrical solutions. Additionally, compatibility with the complementary metal-oxide-semiconductor (CMOS) processes provides the potential for low-cost mass production. These advantages have fostered a new generation of high-performance silicon photonic devices such as waveguides, filters, modulators, switches, and photodetectors for photonic interconnection networks [1]–[5].

Devices based on microring resonators are attractive as the building blocks for on-chip interconnect systems. In particular, the electrooptic broadband microring switch is a compact device that is capable of routing high-bandwidth wavelength-parallel optical messages through a photonic interconnection network [1]. Moreover, electrooptic control of the microring switch enables a more scalable and energy efficient interconnection network compared to the all-optical switching methods that have been demonstrated [1], [2]. Thus far, the microring switch has successfully been shown to be capable of switching high-speed optical data encoded with the on-off-keyed (OOK) format [3].

Manuscript received January 31, 2011; revised March 22, 2011; accepted April 15, 2011. Date of publication April 25, 2011; date of current version July 20, 2011. This work was supported by the National Science Foundation and Semiconductor Research Corporation under Grant ECCS-0903406 SRC Task 2001.

L. Xu, J. Chan, A. Biberman, and K. Bergman are with the Department of Electrical Engineering, Columbia University, New York, NY 10027 USA (e-mail: lx2140@columbia.edu).

H. L. R. Lira and M. Lipson are with the School of Electrical and Computer Engineering, Cornell University, Ithaca, NY 14853 USA.

Color versions of one or more of the figures in this letter are available online at <http://ieeexplore.ieee.org>.

Digital Object Identifier 10.1109/LPT.2011.2147300

Although silicon microring modulators encode optical data onto individual wavelength channels in a wavelength-division-multiplexed system [6], the total available bandwidth in the optical transmission system is ultimately limited by the free spectral range (FSR) of the resonator in the modulator [7]. By moving toward advanced modulation formats such as multilevel signaling, we enable another dimension for scaling the bandwidth, while maintaining the same FSR of the resonator. The use of multilevel OOK format is challenging since the threshold power will vary according to the optical path a signal travels through [8]. However, advanced modulation formats such as quadrature phase-shift keying avoid this varied path-length ambiguity by separating the quadrature components before detection. The generation of phase-shift-keyed (PSK) formats using the microring resonator has been proposed [9], [10], and experimentally demonstrated [11].

Differential-phase-shift-keyed (DPSK) format exhibits several advantageous qualities. It enables 3-dB improved receiver sensitivity with balanced detection, and has higher tolerance to nonlinear degradation compared with OOK. Moreover, an extension to multilevel modulation formats enables higher data bandwidth. Despite the recent interest in PSK format for optical communication systems, the electrooptic switching of PSK signals using silicon photonic microring resonators has yet to be demonstrated. This limitation is due to the frequency discriminator behavior of microrings on PSK signals, where phase information is transformed into intensity information as the result of the resonator's narrow bandpass behavior [12], [13].

To reduce the discriminator behavior, a second-order microring resonator may be employed since it possesses a wider and flatter passband than the single-order microring [4], [12]. In this work, we experimentally demonstrate for the first time the transmission of single- and multichannel 10-Gb/s DPSK optical signals through a second-order electrooptic microring switch, showcasing high-bandwidth routing of optical PSK signals with fast switching transitions, high extinction ratios, and low driving voltage. We confirm format transparency of the microring switch for the PSK format, and validate the use of DPSK signaling for photonic interconnection networks.

II. DEVICE CHARACTERIZATION

The device used in this experiment (Fig. 1(a)) is a second-order 1×2 switch consisting of two microring resonators, coupled together and to two adjacent waveguides, similar to the switch demonstrated in [3], [4]. By injecting electrical carriers into one of the microring cavities through a PIN diode, the corresponding resonance is tuned. This electrical control allows an optical signal to be switched to either the through port (off resonance) or drop port (on resonance). Fig. 1(b) shows the output spectrum of the resonant response for this device for the two

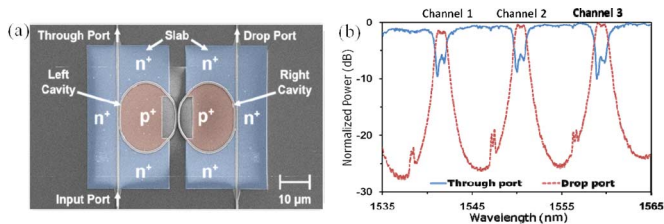


Fig. 1. (a) Top-view scanning-electron-microscope (SEM) image of the device, and (b) spectrum of the resonant response of the device in the passive state.

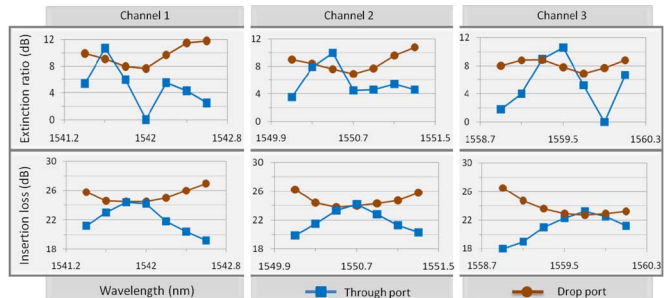


Fig. 2. Measured insertion losses and extinction ratios at different wavelengths in the active state.

output ports in the passive state, before being electrically driven, showing a 9-nm FSR and through-port passbands with 3-dB bandwidths of 85 GHz. The passbands of the two microring cavities are not perfectly overlapping in the passive state with the absence of the electrical bias; these passbands are aligned with the applied voltage bias during active switching, and has been shown to achieve extinction ratios greater than 20 dB [4].

To demonstrate active switching of multiple DPSK wavelength channels, we first scan a CW lightwave across each resonance to measure the extinction ratio of the gating for both output ports. The optical signal is either switched to through port, with a high voltage electric driving signal, or drop port, with a low voltage electric driving signal. Here, we actively switch the device with a $0.8\text{-}V_{PP}$ square wave with a 1.1-V voltage bias, and a 100-ns period with a 50% duty cycle, producing 50-ns optical data packets at both output ports. The measured insertion losses and extinction ratios for both output ports at different wavelengths are shown in Fig. 2. The three transmission wavelengths used in the experiment are chosen to be 1541.6 nm, 1550.4 nm, and 1559.3 nm. The wavelength selection is based on optimal and balanced extinction ratios across the through and drop ports, and therefore they do not coincide with the wavelength of the optimal insertion loss. The variations in extinction ratios at the above wavelengths are caused by the interaction of the resonances of the two microrings and the optical power sent to the EDFA.

III. EXPERIMENT

The experimental setup is shown in Fig. 3. Two CW lightwaves, centered at 1550.4 nm and 1559.3 nm, are generated using distributed feedback (DFB) laser sources, and a third CW lightwave centered at 1541.6 nm is generated by a tunable laser (TL) source. They are combined using an arrayed waveguide grating (AWG), and are aligned to the same polarization using polarization controllers (PC). The lightwaves are then modulated using a phase modulator (PM) driven with a 10-Gb/s, 2^7-1

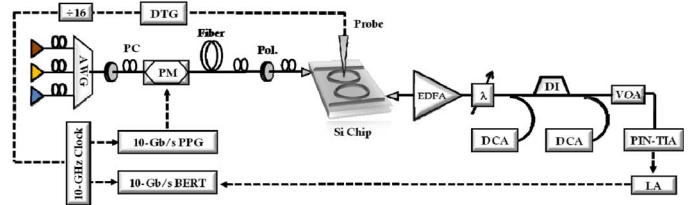


Fig. 3. Experimental setup using the silicon electrooptic microring switch. Solid line: optical link. Dashed line: electrical link.

pseudorandom bit sequence (PRBS) pattern from a pulse pattern generator (PPG) to generate a DPSK signals, and are then desynchronized on bit level using 500-m standard single-mode optical fiber. The operation and performance of the microring switch is independent to the transmitted data pattern, as long as the occupied spectrum of the transmitted signal is the same. The optical signals pass through a polarizer and then couple into the on-chip nano-tapered silicon waveguide using a tapered fiber. A data timing generator (DTG) switches the device by contacting the silicon chip with high-speed RF probes.

The optical signals egressing from the chip pass through an erbium-doped fiber amplifier (EDFA), filter (λ), delay interferometer (DI), and variable optical attenuator (VOA). The signals are detected using a photodetector (PIN-TIA) followed by a limiting amplifier (LA), and examined on a bit-error rate tester (BERT). The DTG gates the BERT over the duration of each optical packet. All the clock sources are synchronized. An optical spectrum analyzer and a DCA are used to evaluate the spectral and temporal performance, respectively. The BERT external gating window is set to 41 ns for signals egressing from the through port, and 35 ns for signals egressing from the drop port, ensuring that the data portion of the packet is measured without the packet transients, roll-off, and overshoot. The external gating window is different for the two ports due to the performance variation. We measure the back-to-back BER curve of the packetized DPSK signal bypassing the chip, gated using an external modulator and set to 11-dB extinction ratio. It is attenuated to the corresponding optical power in the previous experiment before entering the EDFA, and measured with the same experimental setup used to investigate signal degradation caused by the microring switch.

IV. RESULTS

A. Single Channel Switch

We switch a single wavelength channel encoded with 10-Gb/s DPSK signal, and record optical data packets, including their rising and falling edges, at each output port of the switch before and after the DI (Fig. 4(a)–(c)). The rising and falling time (10% and 90% of the signal, respectively) are 0.86 and 3.67 ns for through port; 1.87 and 0.8 ns for drop port, respectively. The total average optical power injected into the silicon chip is 0 dBm. BER measurements (Fig. 4(d)) on the packetized data at each output port of the switch and back-to-back case bypassing the silicon chip are achieved with error-free operation (defined as having BERs less than 10^{-12}). The BER curves overlap for switched signals egressing from the drop and through port, and a 1.4-dB power penalty is observed compared to the back-to-back case. The power penalty

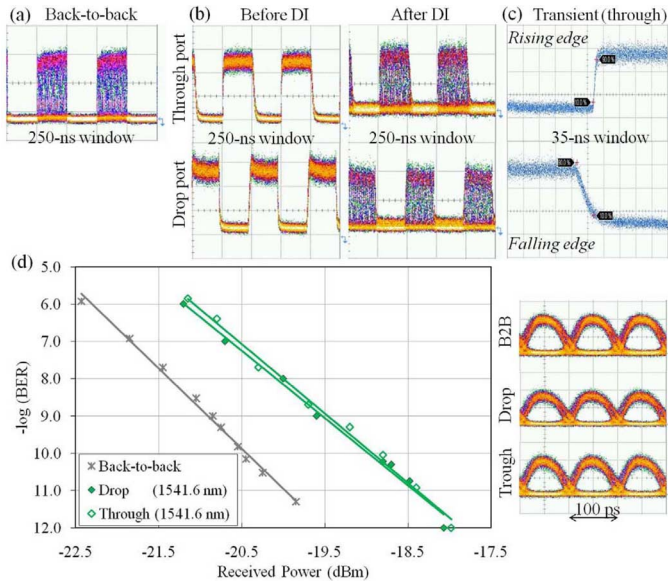


Fig. 4. (a) Back-to-back optical packets bypassing the chip gated using external modulator after DI. (b) Output optical packets before and after DI for both output ports. (c) Transients for through port before DI. (d) Left: BER curves for single-channel switch. Right: respective eye diagrams.

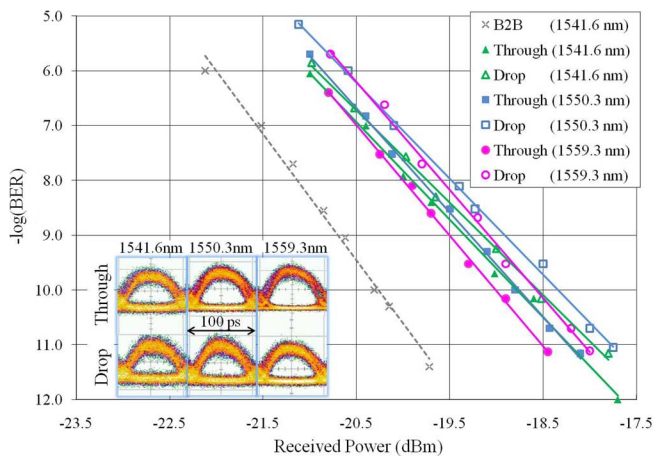


Fig. 5. BER curves for multichannel switch. Inset: respective eye diagrams.

mainly comes from partial filtering effect from the nonflat top passband, and asymmetric resonance profile of the microring resonator, which degrade the phase encoded signal. DPSK exhibits less tolerance to filtering effects than OOK signals, which accounts for the increased power penalty.

B. Multichannel Switch

In multichannel configuration, the three wavelength channels are switched between the drop and through port simultaneously. The total average optical power injected into the silicon chip is 2 dBm, equally distributed among the three wavelength channels, before entering the waveguide. BER measurements are performed on the packetized data at each output port of the switch, as well as the back-to-back case bypassing the silicon chip, observing error-free operation (Fig. 5). Eye-diagrams for the drop and through port at different wavelengths are shown in the Fig. 5 inset. All the monitored channels have similar performance characteristics, which are summarized in Table I. Additional power penalties for wavelength channels at the drop ports

TABLE I
SUMMARY OF MULTICHANNEL SWITCH RESULTS

Wavelength (nm)	Through Port		Drop Port	
	Extinction Ratio (dB)	Power Penalty (dB)	Extinction Ratio (dB)	Power Penalty (dB)
1541.6	10.7	1.3	9.1	1.5
1550.4	9.0	1.3	8.0	1.7
1559.3	9.0	1.1	8.9	1.5

compared to the through ports are attributed to lower power going into the EDFA.

V. CONCLUSION

We have demonstrated and characterized the transmission of 10-Gb/s DPSK signals through a silicon microring electrooptic switch, and observed error-free operation for drop and through port in both the single- and multiwavelength-channel configurations. These empirical validations confirm the suitability of the microring switch for varying modulation formats, enabling the option of DPSK signaling, and potentially its multilevel modulation formats, for next-generation photonic interconnection networks.

REFERENCES

- [1] B. G. Lee, A. Biberman, P. Dong, M. Lipson, and K. Bergman, "All-optical comb switch for multiwavelength message routing in silicon photonic networks," *IEEE Photon. Technol. Lett.*, vol. 20, no. 10, pp. 767–769, May 2008.
- [2] Y. Vlasov, W. M. J. Green, and F. Xia, "High-throughput silicon nanophotonic wavelength-insensitive switch for on-chip optical networks," *Nature Photon.*, vol. 2, pp. 242–246, Apr. 2008.
- [3] A. Biberman, H. L. R. Lira, K. Padmaraju, N. Ophir, M. Lipson, and K. Bergman, "Broadband CMOS-compatible silicon photonic electro-optic switch," in *Proc. Conf. Lasers and Electro-Optics*, May 2010, Paper CPDA11.
- [4] H. L. R. Lira, S. Manipatruni, and M. Lipson, "Broadband hitless silicon electro-optic switch for on-chip optical networks," *Opt. Express*, vol. 17, no. 25, pp. 22271–22280, Dec. 2009.
- [5] Q. Xu, S. Manipatruni, B. Schmidt, J. Shakya, and M. Lipson, "12.5 Gbit/s carrier-injection-based silicon micro-ring silicon modulators," *Opt. Express*, vol. 15, no. 2, pp. 430–436, Jan. 2007.
- [6] Q. Xu, B. Schmidt, J. Shakya, and M. Lipson, "Cascaded silicon microring modulators for WDM optical interconnection," *Opt. Express*, vol. 14, no. 20, pp. 9430–9435, Oct. 2006.
- [7] Q. Xu, D. Fattal, and R. G. Beausoleil, "Silicon microring resonators with 1.5- μm radius," *Opt. Express*, vol. 16, no. 6, pp. 4309–4315, Oct. 2008.
- [8] J. Chan, G. Hendry, A. Biberman, and K. Bergman, "Architectural exploration of chip-scale photonic interconnection network designs using physical-layer analysis," *J. Lightw. Technol.*, vol. 28, no. 9, pp. 1305–1315, May 1, 2010.
- [9] L. Zhang, J. Y. Yang, M. Song, Y. Li, B. Zhang, R. G. Beausoleil, and A. E. Willner, "Microring-based modulation and demodulation of DPSK signal," *Opt. Express*, vol. 15, no. 18, pp. 11564–11569, Sep. 2007.
- [10] L. Zhang, J. Y. Yang, Y. C. Li, M. P. Song, R. G. Beausoleil, and A. E. Willner, "Monolithic modulator and demodulator of differential quadrature phase-shift keying signals based on silicon microrings," *Opt. Lett.*, vol. 33, no. 13, pp. 1428–1430, Jul. 2008.
- [11] K. Padmaraju, N. Ophir, S. Manipatruni, C. B. Poitras, M. Lipson, and K. Bergman, "DPSK modulation using a microring modulator," in *Proc. Conf. Lasers and Electro-Optics*, Baltimore, MD, May 2011, Paper CTuN4.
- [12] L. Xu, C. Li, C. Y. Wong, and H. K. Tsang, "Optical differential-phase-shift-keying demodulation using a silicon microring resonator," *IEEE Photon. Technol. Lett.*, vol. 21, no. 5, pp. 295–297, Mar. 1, 2009.
- [13] L. Xu, C. Li, C. Y. Wong, and H. K. Tsang, "DQPSK demodulation using integrated silicon microring resonators," *Opt. Commun.*, vol. 284, no. 1, pp. 172–175, Jan. 2011.